Dislocation relaxation peaks involving hydrogen drag in deformed Ni-H alloys

K. Tanaka, T. Inukai, K. Uchida, and M. Yamada
Department of Metallurgical Engineering, Nagoya Institute of Technology, Showa-ku, Nagoya 466, Japan

(Received 22 April 1983; accepted for publication 28 July 1983)

The internal friction and modulus changes in pure and hydrogenated nickel are measured after plastic deformation at frequencies of 2 Hz and 30 kHz. The hydrogen dissolution strongly diminishes a Bordoni-type peak (B peak) but develops a Snoek–Köster-type peak (SK peak) at a temperature well above the B peak. The SK peak increases in height and shifts toward higher temperature with increasing hydrogen concentration up to 1600 at. ppm. It has an effective activation enthalpy of 0.50 ± 0.05 eV. An analysis of the concentration dependence of the peak shift suggests that this peak is caused by dislocations dragging pairs of hydrogen atoms, rather than isolated ones, segregated in the vicinity of the dislocations. A simple model is proposed which involves both dislocation pinning and impurity drag with changes in temperature. It explains well the observed correlation between the B peak and the SK peak as well as the conservation of their total relaxation strength with changes in the hydrogen concentration.

PACS numbers: 62.40. + i, 61.70.Le

I. INTRODUCTION

The behavior of hydrogen dissolved in metals has attracted a large number of experimental and theoretical studies in the past.[1] Hydrogen is readily introduced into a metal lattice either through a cathodic reaction in an electrolyte solution or through equilibration with the gas phase at appropriate temperatures and pressures followed by rapid quenching. It penetrates fairly quickly into the lattice by interstitial diffusion and in due time a uniform solid solution is formed. A part of the absorbed hydrogen however may be trapped by lattice defects such as vacancies, foreign atoms, dislocations, and (sub)grain boundaries or may precipitate as metal hydrides, which results in affecting the physical properties of the metal significantly. The presence of dissolved hydrogen can be detected by mechanical testing, transmission electron microscopy, and many other experimental techniques for measuring the physical properties of metals including the internal friction.[2] An internal friction study in nickel-hydrogen alloys is reported in this paper.

In our previous paper,[3] the effect of hydrogen charging on the internal friction in plastically deformed nickel was reported, and it was shown that the dissolved hydrogen strongly suppresses an intrinsic dislocation peak P_d but instead causes another peak P_{dH} at a higher temperature. The former was ascribed to the Bordoni-type while the latter to the Snoek–Köster-type relaxation peaks in nickel. In a subsequent paper,[4] where the technique of cathodic charging at 323 K was used, some anomalous annealing characteristics of P_{dH} were reported, and it was concluded that the anomaly is primarily caused by the initially nonuniform distribution of hydrogen within the specimens investigated.

In the present study, we therefore attempt to reexamine the behavior of these peaks for specimens containing controlled amounts of hydrogen in uniform solid solutions. To attain this purpose, hydrogenation by the gas absorption technique is employed, which enables us to vary the hydrogen content widely from 4 up to 1600 at. ppm as described in the next section. We are chiefly interested in the concentration dependence of the peak temperatures and peak heights of P_d and P_{dH}. Damping mechanisms causing these two types of peaks are discussed in relation with current theoretical models of dislocation relaxations in the presence of foreign atoms.[5–9]

II. EXPERIMENTAL PROCEDURE

Nickel specimens (purity $\geqslant$99.95 wt. %) in the form of wires of 3 and 1 mm Φ we prepared in the same way as described previously.[3] Hydrogenation was carried out as follows. For specimens of relatively low hydrogen contents ($C_H \leqslant 370$ at. ppm), the apparatus shown in Fig. 1(a) was used. It consists of a Sieverts' type apparatus connected with a vertical furnace used for quenching a specimen into cold mercury. A gas pressure normally below 1 atm was precisely measured with a mercury or an oil manometer. Lower pressures down to 10^{-4} atm were obtained by partitioning. The equilibrating temperature was kept at 973 K. This apparatus could also be used for quenching in vacuum of better than 1×10^{-6} Torr as well as for the analysis of hydrogen content by the gas extraction technique. For specimens of relatively high hydrogen contents ($370 < C_H \leqslant 1600$ at. ppm), the separate apparatus shown in Fig. 1(b) was used. A specimen was set inside a thin stainless-steel holder, one end being sealed and the other end linked to a pressure gauge with a thin stainless-steel tube. The specimen was heated to 773 K in vacuum and a high-purity hydrogen gas of a pressure of 1–50 atm was supplied. Quenching was performed by directly inserting the holder into cold water.

Figure 2 shows a log-log plot of pressure P (atm) versus hydrogen content C_H (at. ppm) obtained for a standard specimen at 773 and 973 K. It is clear from this figure that the data well satisfy the Sieverts' law

$$C_H = K P^{1/2} \exp\left(-\frac{Q_s}{kT}\right), \tag{1}$$

where K is a constant, Q_s the heat of solution per H atom, k the Boltzmann's constant, and T the temperature. Least-squares fitting to Eq. (1) gives the results $K = 2730$ and $Q_s = 0.16$ eV, which are in reasonable agreement with pub-

 0021-8979/83/126890-07$02.40

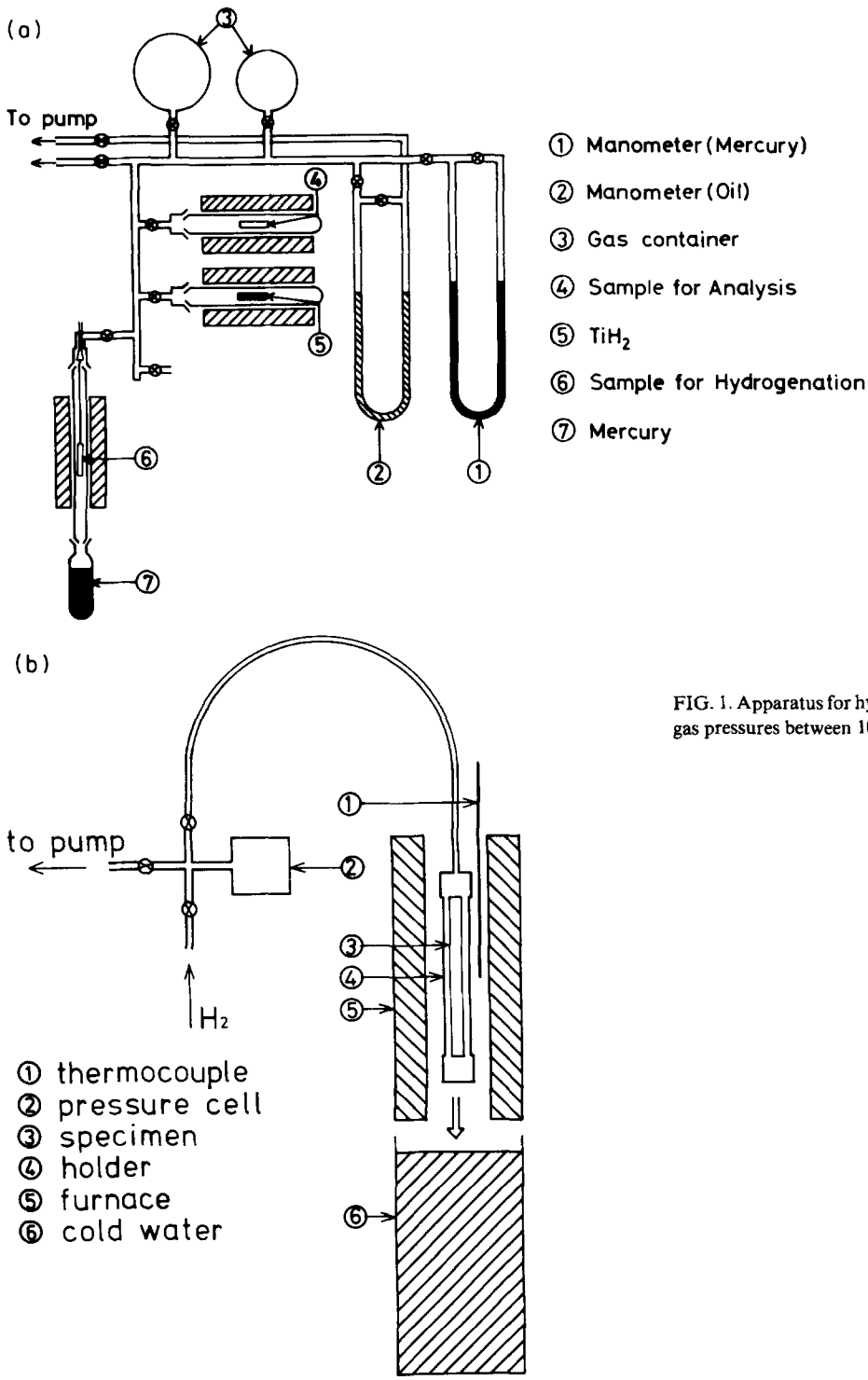

FIG. 1. Apparatus for hydrogenation by gas absorption techniques; (a) H_2 gas pressures between 10^{-4} and 1 atm, and (b) between 1 and 50 atm.

lished results.[10] We then obtain $C_H = 373\,P^{1/2}$ at 973 K, and $C_H = 222\,P^{1/2}$ at 773 K. These relationships were used to evaluate C_H throughout this work.

The hydrogenated specimens were elongated by 5%–8% at room temperature at a strain rate of 2×10^{-4} s^{-1}. Small serrations were frequently observed in the stress-strain curves of heavily-charged specimens. In Fig. 3 are plotted 0.2% proof stress and 5% flow stress against C_H for several specimens (3 mm Φ) used for the internal friction measurements. They are found to be rather insensitive to the hydrogenation except that the 5% flow stress shows a slight initial increase with C_H.

Internal friction measurements were carried out in torsional and longitudinal modes of vibration.[3] A computer-controlled system was used for the measurements in torsional vibration. An external dc magnetic field of 500 Oe was applied for the measurements in longitudinal vibration to minimize the magnetomechanical and eddy-current losses which caused a considerably high background damping especially in the high-frequency range[11]; the former loss was

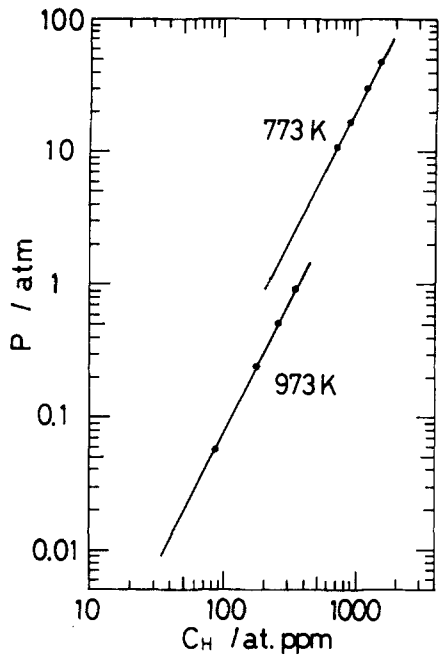

FIG. 2. Relations between H_2 gas pressure P and dissolved hydrogen content C_H in nickel at 773 and 973 K.

able to be suppressed by plastic deformation but the latter was not. In the low-frequency range, only the magnetomechanical loss was significant in annealed specimens, but it was readily eliminated by a small plastic strain. The measurements in torsional vibration were therefore carried out without applying external magnetic field.

III. RESULTS

Figure 4 shows internal friction spectra of a pure and several hydrogenated specimens measured in torsional vibration (~2 Hz) after elongation by about 8%. A peak P_d accompanied by a small subsidiary one is observed at about 90 K in the pure specimen. Dissolution of only 10 at. ppm hydrogen raises the upper tail of P_d implying the emergence of an additional peak. A further increase in C_H greatly reduces the height of P_d but instead develops a new peak P_{dH}

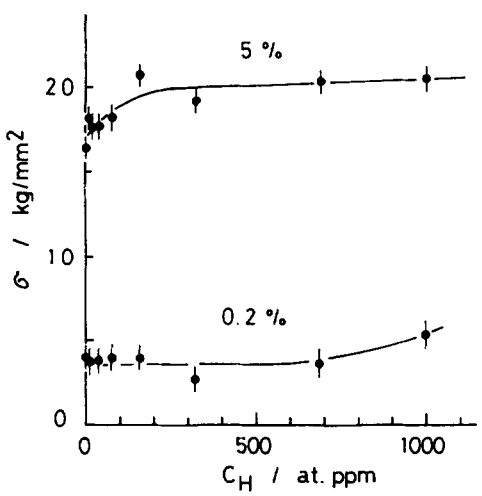

FIG. 3. Proof stress at 0.2% strain and flow stress at 5% strain plotted against dissolved hydrogen content C_H.

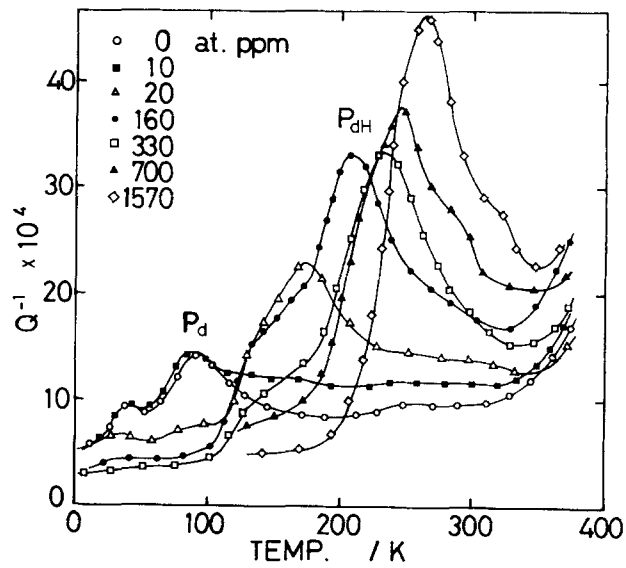

FIG. 4. Internal friction spectra of pure and hydrogenated specimens measured in torsional vibration at frequencies of ~2 Hz after elongation by ~8%.

at a temperature well above P_d; note that both peaks coexist in this stage. P_{dH} continues to grow and shift toward higher temperature with increasing C_H up to 1570 at. ppm where P_d has been completely suppressed.

Both these peaks are of the relaxation type and have the corresponding modulus defects as revealed in the data of frequency change shown in Fig. 5; the peak positions of P_d and P_{dH} are marked with filled and open triangles, respectively. It is evident from this figure that the modulus defect of P_d is suppressed while that of P_{dH} is enhanced with in-

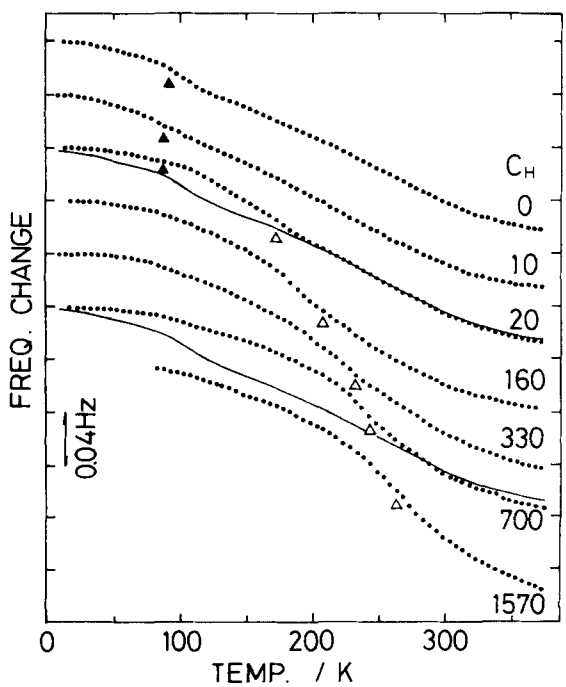

FIG. 5. Frequency changes corresponding to the internal friction spectra shown in Fig. 4. The peak positions of P_d and P_{dH} are marked with filled and open triangles, respectively. Solid curves represent the frequency change of the pure specimen.

creasing C_H. It has already been confirmed that the net modulus change is nearly conserved in a deformed nickel specimen before and after electrolytic charging.[3] This conservation also holds in some of the present specimens as shown in the figure; compare with the frequency change of the pure specimen (thin solid curves). However, some deviations from the conservation rule occur in the other specimens, which might suggest that the dislocation substructures in deformed specimens change somewhat depending upon the amount of dissolved hydrogen even if the degrees of deformation are similar. It must be added here that, though the peak temperature of P_{dH} depends strongly upon C_H, it is rather insensitive to the amount of deformation and hence to changes in the substructure; the peak shift of P_d is always much less.

Figure 6 shows internal friction spectra of pure and hydrogenated specimens measured in longitudinal vibration (~ 30 kHz) after elongation by 5%. Only a low-temperature peak P_d can be seen in the pure specimen. This peak is greatly reduced while another peak P_{dH} is developed with addition of a trace of hydrogen. With increasing C_H the former goes on decreasing while the latter shows up shifting toward higher temperature; both peaks coexist as long as C_H stays below 40 at. ppm, beyond which P_d disappears and only P_{dH} remains.

The modulus defects corresponding to these peaks changed with C_H similarly to those observed in the measurements of torsional vibration (Fig. 5). The strongly correlated behavior of P_d and P_{dH} mentioned above is quite consistent with that shown in Fig. 4. It is therefore concluded that these two types of peaks are governed by two distinct but mutually correlated mechanisms which prevail equally in both low- and high-frequency measurements.

Before proceeding to the discussion of the results, a few additional remarks deserve to be made:

(1) P_{dH} is caused only in the presence of plastic deformation and hydrogen. As shown in Fig. 7 for longitudinal vibration, neither P_d nor P_{dH} appears in as-annealed, hydrogen-free ($C_H = 0$), and hydrogenated ($C_H = 340$ and 1620) specimens; only a small and broad damping peak due to eddy-current loss can be seen.[11] A pronounced peak P_{dH} was really confirmed to develop after 5% elongation in the hydrogenated specimens.

(2) P_{dH} monotonically decays and shifts downwards during annealing at 373 K. No anomalous annealing behavior, i.e., growth and subsequent decay of the peak height observed previously,[3,4] took place in the present study because of the uniform distribution of hydrogen within the specimens investigated. This annealing effect is no doubt associated with the desorption of hydrogen from the specimens.

(3) As C_H approaches 1000 at. ppm or above, the temperature of P_{dH} in the measurements at high frequency is in the range of 373 K or above, where a decrease in hydrogen content would take place and hence the precise determination of the peak temperature and peak strength might not be possible.

(4) The magnitudes of the internal friction presented in Figs. 4 and 6 differ by a factor of about five from each other. The cause of this discrepancy is not clear, but it may partly be attributed to the difference in vibrational modes (torsional and longitudinal) for measuring the internal friction of elongated specimens.

In Fig. 8 the logarithm of C_H is plotted against reciprocal peak temperature of P_{dH} for the measurements at 2 Hz and 30 kHz. One finds from this figure that a linear relation exists between the two quantities, which is expressible as

$$\ln C_H = A(\omega) - \frac{Q}{kT}, \tag{2}$$

where ω is the angular frequency. Least-squares fitting gives $Q = 0.22 \pm 0.03$ eV for both frequencies. Upward devia-

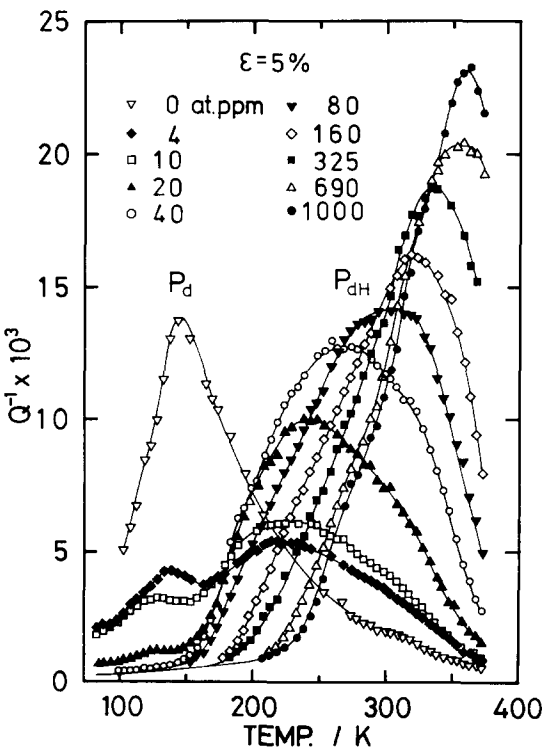

FIG. 6. Internal friction spectra of pure and hydrogenated specimens measured in longitudinal vibration at frequencies of ~ 30 kHz after elongation by 5%.

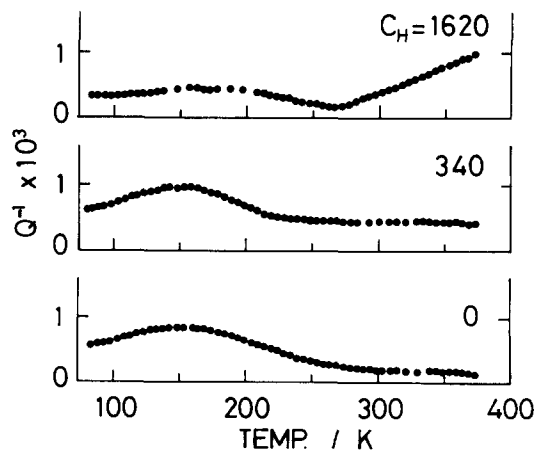

FIG. 7. Internal friction spectra of pure and hydrogenated specimens without deformation measured in longitudinal vibration.

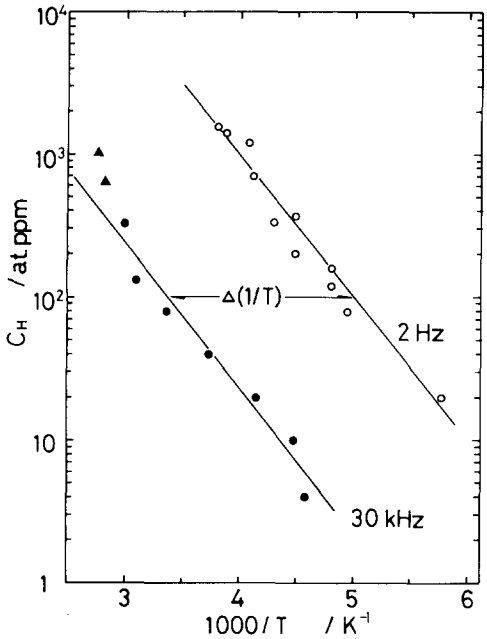

FIG. 8. Logarithm of C_H plotted against reciprocal peak temperature of P_{dH} for the measurements at 2 Hz and 30 kHz.

tions from this Arrhenius relationship are seen when the peak temperatures approach and exceed 373 K (data points marked with filled triangles). This deviation is probably related with the effect mentioned above in remark (3) and hence these data points have been omitted in the evaluation of Q. Now, we define the effective activation enthalpy for P_{dH} by

$$H_{\text{eff}} = k\left(\frac{\partial \ln \tau}{\partial(1/T)}\right)_{C_H}, \tag{3}$$

where τ is the relaxation time. Utilizing the relationship $\omega\tau = 1$ at the peak temperature and noting that the peak shift $\Delta(1/T)$ corresponding to the change in logarithmic frequency $\Delta \ln \omega$ is given by the lateral separation between the two parallel lines as shown in the figure, we obtain $H_{\text{eff}} = 0.50 \pm 0.05$ eV irrespective of C_H.

IV. DISCUSSION

The general features of the internal friction and modulus changes in deformed Ni-H alloys described above are in qualitative agreement with those found in the previous studies,[3,4] except that the hydrogen content is specified to every specimen investigated in the present study. In accordance with the previous interpretation, it seems most appropriate to assign P_d to the Bordoni-type relaxation peak (B peak) which is associated with an intrinsic dislocation motion overcoming Peierls valleys by thermally activated kink-pair formation, while P_{dH} to the Snoek–Köster-type relaxation peak (SK peak) which has its origin in an interaction between hydrogen atoms and dislocations in deformed nickel. Several realistic models for the SK peak have hitherto been proposed, of which the dislocation relaxation mechanisms involving impurity drag[5–9] appear to be most relevant to the cause of P_{dH}.

Schoeck[5] proposed a mechanism based on the string model in which were included dislocations oscillating in an impurity cloud, and derived the relaxation time and the relaxation strength Δ given by

$$\tau = \alpha \frac{kT}{Gb^3} \frac{C_d l^2}{D} \tag{4}$$

and

$$\Delta = \beta \Lambda l^2 . \tag{5}$$

In the above formulas, α and β are numerical constants of order 1 and 0.1, respectively, G the shear modulus, b the dislocation strength, l the segment length of a dislocation, Λ the dislocation density, C_d the concentration of impurity atoms along the dislocation, and D the diffusion coefficient of the impurity atoms dragged by the dislocation. Recently, essentially equivalent formulas to the above have been derived by Lücke and Granato[8] based on their original equation of dislocation damping.[12] Since D is expressible as $D = D_0 \exp(-H_m/kT)$, where H_m is the migrational enthalpy of the impurity atoms along with the dislocation motion, τ is rewritten as

$$\tau = \alpha \frac{kT}{Gb^3} \frac{l^2}{D_0} C_d \exp\left(\frac{H_m}{kT}\right). \tag{6}$$

Seeger[6] proposed a different mechanism based on the kink model in which were involved the formation and sideway diffusion of kink pairs along a dislocation dragging impurity atoms, and derived expressions for τ and Δ. He examined several limiting cases for the combination of the kink density and the impurity concentration at the dislocation.[7] The simplest expression for the relaxation time for the above process is given by

$$\tau = \gamma kTC_d \exp\left(\frac{2H_k + H_m}{kT}\right), \tag{7}$$

where γ is a parameter including l but virtually independent of T and C_d, and H_k is the formation enthalpy of an isolated kink. An expression equivalent to Eq. (5) was derived for the relaxation strength.

It is important to note that in any of the above theoretical models τ is indicated to be proportional to $C_d T$. It seems therefore reasonable to assume that the relaxation time of P_{dH} is written as

$$\tau = \rho TC_d \exp\left(\frac{H_r}{kT}\right), \tag{8}$$

where ρ is a parameter independent of T and C_d. There remain certain ambiguities regarding the temperature and concentration dependence of C_d. Miner *et al.*[13] made a detailed analysis of the SK peak in bcc Fe-C (or N) alloys based on Schoeck's model and showed that H_{eff} for the SK peak could reasonably be explained if C_d was assumed to obey the Fermi–Dirac distribution; for sufficiently low interstitial impurity content, C_d obeys the Boltzmann statistics and becomes proportional to the impurity concentration. However, in Ni-H alloys where the SK peak manifests much stronger concentration dependence of the peak temperature than in the Fe-C(N) alloys, C_d should obey an alternative distribution. We assume that it takes the form

$$C_d = \lambda C_H^n \exp\left(\frac{B}{kT}\right), \tag{9}$$

and try to determine the exponent n consistently. Equation (8) is rewritten as

$$\ln \tau = \ln(\rho\lambda T) + n \ln C_H + \frac{H_r + B}{kT}. \tag{10}$$

Substituting Eq. (10) into Eq. (3) and neglecting a small correction of $\ln(\rho\lambda T)$, we obtain $H_{\text{eff}} = H_r + B$. Furthermore, Eq. (10) reduces to Eq. (2) for a given value of τ if a relation $Q = (H_r + B)/n$ holds. Putting $H_r + B = 0.50 \pm 0.05$ eV and $Q = 0.22 \pm 0.03$ eV gives $n = 2.2 \pm 0.4$.

The physical meaning of $n \simeq 2$ may be understood as follows: Pairs of hydrogen atoms which are in thermal equilibrium with free isolated ones and are segregated in the vicinity of a dislocation, are most effectively dragged by the dislocation in nickel. The parameter B is then identified as the net binding energy of the pair itself and between the pair and the dislocation. The lower limit of B can be estimated from the condition that P_d disappears for C_H above a critical concentration because of locking of dislocations by the pairs. This condition may be met, e.g., for $C_d \gtrsim 5\times10^{-3}$ with $C_H = 40\times10^{-6}$ and $T = 130$ K, resulting in $B \geqslant 0.14$ eV ($\lambda \sim 10$ is assumed). Adopting, for example, $B = 0.14$ eV and noting that $H_r = H_m$ in terms of Schoeck's model, we obtain $H_m = 0.36 \pm 0.05$ eV. This value is comparable with the activation energy 0.41 eV for hydrogen diffusion in nickel measured above room temperature.[14] On the other hand, Seeger's model indicates $H_r = 2H_k + H_m$. Adopting $2H_k = 0.16$ eV,[3,15] which corresponds to the activation enthalpy of P_d, leads to $H_m = 0.20 \pm 0.05$ eV. This value is much smaller than the energy for diffusion referred to above, but it is noteworthy that Combette *et al.*[16] have suggested a similar diffusional energy, $H_m = 0.19$ eV, from an analysis of hydrogen segregation to dislocations at temperatures between 110 and 170 K in deformed nickel. More elaborate study is necessary to clarify the atomistic process involved in the relaxation mechanism of P_{dH}.

We next discuss the interrelation between the relaxation strengths of P_d and P_{dH}. It is evident from Eq. (5) that Δ of the SK peak is independent of C_H in both above models. However, this is in strong contrast with the experimental observation on P_{dH}, the strength of which manifests a definite concentration dependence. An idea is proposed below which well explains the behavior of P_d and P_{dH} with changes in the hydrogen concentration.

Consider a dislocation segment lying along a Peierls valley in a crystal as sketched in Fig. 9. (a) With no pinning points, it bows out under oscillating stress of fixed amplitude by repeatedly creating and expanding kink pairs, and causes the B peak at a low temperature whose strength is proportional to the maximum area swept by the dislocation segment. (b) When a low density of pinning points is added to the dislocation, its motion is restricted and the strength of the B peak is rapidly decreased. However, these pinning points can be dragged by the dislocation at elevated temperatures until the same area as in (a) is reached, which causes an additional peak, the SK peak, whose strength is proportional

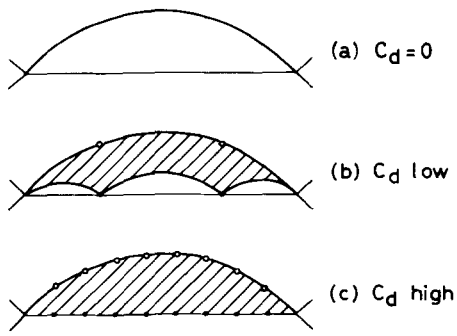

FIG. 9. Straight dislocation segments with and without pinning points between firmly locked ends. Under a shear stress they bow out to balance their line tension. The pinning points are dragged by the dislocations at elevated temperatures.

to the additionally swept area (hatched region). Under this condition both B and SK peaks coexist though the sum of their strengths is always conserved. (c) With a high enough density of pinning points, the B peak disappears while the SK peak reaches its maximum strength.

This model, though very intuitive at the present stage, is supported by some of our experimental observations:

(1) It accounts well for the observed interrelation between P_d and P_{dH} with changes in C_H.

(2) It also accounts for the conservation rule of net modulus change as mentioned previously.

(3) It predicts the conservation of total relaxation strength of P_d and P_{dH} with changes in C_H, in agreement with the experiment as shown below.

We define the relaxation strengths of the B and SK peaks by Δ_B and Δ_{SK}, respectively. These parameters cannot be directly obtained from the peak heights of P_d and P_{dH}, because these peaks are much broader than a single Debye peak and hence expected to consist of wide distributions of relaxation times. However, the integrated relaxation strengths can be evaluated from the areas, S_B and S_{SK}, of the peaks plotted against inverse temperature if average activation enthalpies, H_B and H_{SK}, are known. Instead of separating into S_B and S_{SK}, we consider the total area $S = S_B + S_{SK}$. Reminding of the fact that the area of a Debye peak is given by $\pi k\delta/2H$, where δ is the relaxation strength and H is the activation enthalpy of the peak, one arrives at the expression

$$S = \frac{\pi k}{2}\left(\frac{\Delta_B}{H_B} + \frac{\Delta_{SK}}{H_{SK}}\right). \tag{11}$$

Since the above model requires that

$$\Delta_B + \Delta_{SK} = \Delta_0 \text{ (constant)}, \tag{12}$$

S is rewritten as

$$S = \frac{\pi k}{2H_{SK}}\Delta_0\left[f_{SK} + \frac{H_{SK}}{H_B}(1 - f_{SK})\right], \tag{13}$$

where $f_{SK} = \Delta_{SK}/\Delta_0$ is the fraction of the relaxation strength of the SK peak. Putting $H_{SK}/H_B = 0.50/0.16 = 3.1$, S is expected to decrease monotonically from 1 to about 1/3 of the original value as f_{SK} increases from 0 to 1.

To examine the above relationship, we present, in Fig.

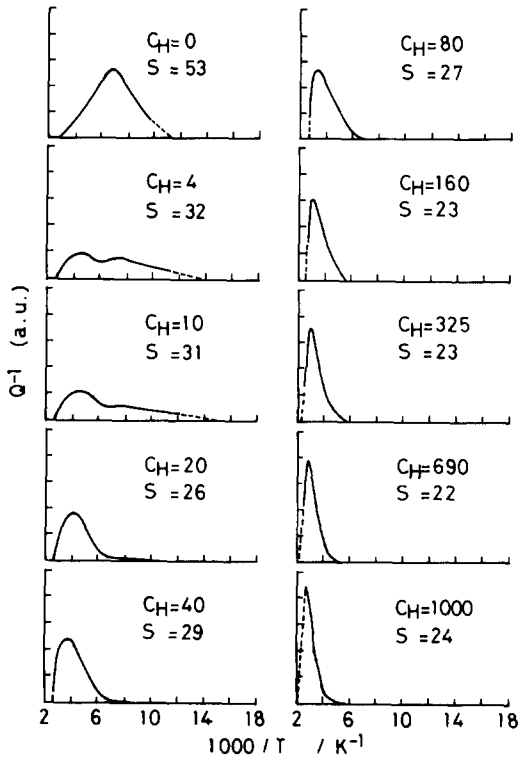

FIG. 10. Internal friction spectra of Fig. 6 redrawn against reciprocal temperature after subtracting their background damping. The area S surrounded by each spectrum is indicated in arbitrary unit.

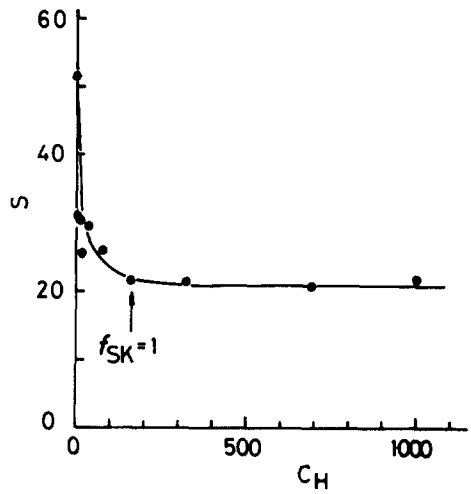

FIG. 11. Area S plotted against C_H.

10, the internal friction spectra of Fig. 6 redrawn against reciprocal temperature after subtracting appropriate background damping. The area S surrounded by each curve is evaluated and indicated in the figure in an arbitrary unit together with C_H. In Fig. 11, S is plotted against C_H. Allowing for unavoidable fluctuation of sample variables other than the hydrogen content, the change in S with C_H appears to be consistent with the above expectation. The hydrogen concentration corresponding to $f_{SK} = 1$ is marked with an arrow in the figure. Note that S becomes nearly unchangeable above this concentration, as expected from the present model.

Granato and Lücke[9] have recently derived the combined effects upon the internal friction and modulus changes which occur when two kinds of drag operate, one acting continually along a dislocation and the other at discrete points (point-defect drag). It has been found that, for widely separated relaxation times, the damping and modulus change can always be expressed in good approximation as the sum of two Debye relaxations, one corresponding to the point-defect drag and the other to continuous drag acting on the inbetween loops.

It is interesting to note that a good analogy seems to exist between our present interpretation and their results—the B peak stands for the continuous drag and the SK peak for the point-defect drag. Further experimental and theoretical studies on these two kinds of peaks are desirable.

[1]See, for example, *Hydrogen in Metals* (I and II), edited by G. Alefeld and J. Völkl (Springer, Berlin, 1978).
[2]J. P. Hirth, Metall. Trans. **11**, A 861 (1980).
[3]K. Tanaka, H. Ryonai, and M. Yamada, J. Appl. Phys. **52**, 3992 (1981).
[4]K. Tanaka, T. Atsumi, and M. Yamada, *Proc. Int. Conf. Internal Friction and Ultrasonic Attenuation in Solids* (ICIFUAS-7, Lausanne, 1981), J. Phys. (Paris) **42**, C5–139 (1981).
[5]G. Schoeck, Acta Metall. **11**, 617 (1963).
[6]A. Seeger, Phys. Status Solidi A **55**, 457 (1979).
[7]A. Seeger, Scr. Metall. **16**, 241 (1982).
[8]K. Lücke and A. V. Granato, Phys. Rev. B **24**, 6991 (1981).
[9]A. V. Granato and K. Lücke, Phys. Rev. B **24**, 7007 (1981).
[10]W. M. Robertson, Z. Metallk. **64**, 436 (1973).
[11]K. Tanaka, T. Kageyama, and T. Mizoguchi, Scr. Metall. **14**, 859 (1980).
[12]A. Granato and K. Lücke, J. Appl. Phys. **27**, 583 (1956).
[13]R. E. Miner, R. Gibala, and F. A. Hultgren, Acta Metall. **24**, 233 (1976).
[14]J. Völkl and G. Alefeld, *Hydrogen in Metals* (I), edited by G. Alefeld and J. Völkl (Springer, Berlin, 1978), p 321.
[15]J. L. Besson and P. Boch, Acta Metall. **26**, 1243 (1978).
[16]P. Combette, M. Renard, and J. Grilhe, Phys. Status Solidi A **11**, 677 (1972).